In this report we solve the boundary value problems for the Helmholtz equation on polygonal domains. We observe that when the problems are formulated as the boundary integral equations of potential theory, the solutions are representable by series of appropriately chosen Bessel functions. In addition to being analytically perspicuous, the resulting expressions lend themselves to the construction of accurate and efficient numerical algorithms. The results are illustrated by a number of numerical examples.

Keywords: *Boundary value problems, Potential theory, Corners, Singular solutions, Helmholz equation, Elliptic partial differential equations*

On the solution of the Helmholtz equation on regions with corners

K. Serkh[‡⋄⊕*], V. Rokhlin[‡⋄⊖],
Technical Report YALEU/DCS/TR-1524
May 11, 2016

⋄ This author's work was supported in part under ONR N00014-11-1-0718, ONR N00014-14-1-0797
⊕ This author's work was supported in part under ONR N00014-10-1-0570 and by the National Defense Science and Engineering Graduate Fellowship
⊖ This author's work was supported in part under AFOSR FA-9550-09-1-0027

‡ Dept. of Mathematics, Yale University, New Haven CT 06511

* Corresponding author. Email: kirill.serkh@yale.edu

On the Solution of the Helmholtz Equation on Regions with Corners

Kirill Serkh and Vladimir Rokhlin

May 11, 2016

Contents

1 Introduction

In potential theory, the Helmholtz equation is reduced to an integral equation by representing the solutions as single-layer or double-layer Helmholtz potentials on the boundaries of the regions. By taking the limit of the solutions to the boundary, the densities of these potentials are shown to satisfy Fredholm integral equations of the *second kind*.

When the boundaries of the regions are smooth, the kernels of the integral equations are weakly singular, and the solutions are also smooth. This environment is well-understood; the existence and uniqueness of the solutions follow from Fredholm's theory, and the integral equations can be solved numerically using standard tools (see, for example, [12]).

When the boundaries of the regions have perfectly sharp corners, both the kernels and the solutions of the integral equations are singular. The behavior in the vicinity of corners of the solutions of both the integral equations and of the underlying differential equation have been the subject of much study (see [31], [16] for representative examples), though the differential equation appears to have recieved more attention than the integral equations. Comprehensive reviews of the literature can be found in (for example) [19], [11].

The leading singular terms in the solutions, in the vicinity of corners, to both the integral and differential equations are known (see, for example, [31]), and there are a number of theorems describing the spaces to which the solutions belong (see, for example, [29], [28]). In 1979, R. J. Riddell published a heuristic argument for the existence of a certain asymptotic series for the solutions to the integral equations near the corners, but this line of investigation does not appear to have been pursued further (see [22]).

In this report, we provide a detailed description of the behavior of the solutions to the integral equations in the vicinity of corners, in the specific case of polygonal boundaries. We observe that the solutions in the vicinity of corners are representable by certain series of appropriately selected Bessel functions. The analytical results are used to construct highly accurate and efficient numerical algorithms, and are demonstrated by a number a numerical examples.

This report is based on several specific analytical observations, which are described in the following section.

2 The Fundamental Observation

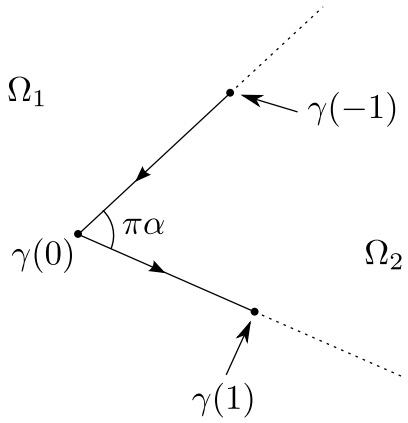

Figure 1: A wedge in $\mathbb{R}^2$

2.1 The Neumann Case

Suppose that $\gamma\colon [-1,1] \to \mathbb{R}^2$ is a wedge in $\mathbb{R}^2$ with a corner at $\gamma(0)$, and with interior angle $\pi\alpha$. Suppose further that γ is parameterized by arc length, and let $\nu(t)$ denote

the inward-facing unit normal to the curve γ at t. Let Γ denote the set $\gamma([-1,1])$. By extending the sides of the wedge to infinity, we divide $\mathbb{R}^2$ into two open sets Ω_1 and Ω_2 (see Figure 1).

Let $\phi\colon \mathbb{R}^2 \setminus \Gamma \to \mathbb{C}$ denote the Helmholtz potential (see, for example, [20]) induced by a charge distribution on γ with density $\rho\colon [-1,1] \to \mathbb{C}$. In other words, let ϕ be defined by the formula

$$\phi(x) = \frac{i}{4} \int_{-1}^{1} H_0(k\|\gamma(t) - x\|)\rho(t)\, dt, \tag{1}$$

for all $x \in \mathbb{R}^2 \setminus \Gamma$, where $\|\cdot\|$ denotes the Euclidean norm. Suppose that $g\colon [-1,1] \to \mathbb{C}$ is defined by the formula

$$g(t) = \lim_{\substack{x \to \gamma(t) \\ x \in \Omega_1}} \frac{\partial \phi(x)}{\partial \nu(t)}, \tag{2}$$

for all $-1 \leq t \leq 1$, i.e. g is the limit of the normal derivative of integral (1) when x approaches the point $\gamma(t)$ from outside. It is well known that

$$g(s) = \frac{1}{2}\rho(s) + \frac{i}{4} \int_{-1}^{1} K(s,t)\rho(t)\, dt, \tag{3}$$

for all $-1 \leq s \leq 1$, where

$$K(s,t) = \frac{k\langle \gamma(s) - \gamma(t), \nu(s) \rangle}{\|\gamma(s) - \gamma(t)\|} H_1(k\|\gamma(s) - \gamma(t)\|), \tag{4}$$

for all $-1 \leq s, t \leq 1$, where $\langle \cdot, \cdot \rangle$ denotes the inner product in $\mathbb{R}^2$(see, for example, [20]).

The following theorem is the first of the two principal results of this section. The

proof can be found in [25].

Theorem 2.1 *Suppose that N is a positive integer and that ρ is defined by the formula*

$$\rho(t) = \sum_{n=1}^{N} b_n(\operatorname{sgn}(t))^{n+1} \frac{J_{\frac{n}{\alpha}}(k|t|)}{|t|} + \sum_{n=1}^{N} c_n(\operatorname{sgn}(t))^n \frac{J_{\frac{n}{2-\alpha}}(k|t|)}{|t|}, \tag{5}$$

for all $-1 \leq t \leq 1$, where $b_1, b_2, \ldots, b_N$ and $c_1, c_2, \ldots, c_N$ are arbitrary complex numbers. Suppose further that g is defined by (3). Then there exist series of complex numbers $\beta_0, \beta_1, \ldots$ and $\gamma_0, \gamma_1, \ldots$ such that

$$g(t) = \sum_{n=0}^{\infty} \beta_n |t|^n + \sum_{n=0}^{\infty} \gamma_n \operatorname{sgn}(t)|t|^n, \tag{6}$$

for all $-1 \leq t \leq 1$. Conversely, suppose that g has the form (6). Suppose further that N is an arbitrary positive integer. Then, for all but finitely many angles $\pi\alpha$, there exist complex numbers $b_1, b_2, \ldots, b_N$ and $c_1, c_2, \ldots, c_N$ such that ρ, defined by (5), solves equation (3) to within an error $O(t^N)$.

In other words, if ρ has the form (5), then g is smooth on the intervals $[-1, 0]$ and $[0, 1]$. Conversely, if g is smooth, then for each positive integer N there exists a solution ρ of the form (5) that solves equation (3) to within an error $O(t^N)$.

Remark 2.1 *Suppose that $G\colon \mathbb{R}^2 \to \mathbb{R}$ solves the Helmholtz equation on a disc containing the wedge $\gamma([-1, 1])$, and that*

$$g(t) = \frac{\partial G}{\partial \nu(t)}(\gamma(t)), \tag{7}$$

for all $-1 \leq t \leq 1$, where $\nu(t)$ is the inward-pointing unit normal vector at $\gamma(t)$. Suppose

further that N is an arbitrary positive integer. In [25] we observe that, for all *angles $\pi\alpha$, there exists a function ρ of the form (5) solving equation (3) to within an error $O(t^N)$.*

Remark 2.2 *The precise relationship between the charge distributions ρ of the form (5) and the boundary data g in equation (3) is described in detail in Appendix A.*

2.2 The Dirichlet Case

Suppose that $\gamma\colon [-1,1] \to \mathbb{R}^2$ is a wedge in $\mathbb{R}^2$ with a corner at $\gamma(0)$, and with interior angle $\pi\alpha$. Suppose further that γ is parameterized by arc length, and let $\nu(t)$ denote the inward-facing unit normal to the curve γ at t. Let Γ denote the set $\gamma([-1,1])$. By extending the sides of the wedge to infinity, we divide $\mathbb{R}^2$ into two open sets Ω_1 and Ω_2 (see Figure 1).

Let $\phi\colon \mathbb{R}^2 \setminus \Gamma \to \mathbb{C}$ denote the Helmholtz potential (see, for example, [20]) induced by a dipole distribution on γ with density $\rho\colon [-1,1] \to \mathbb{C}$. In other words, let ϕ be defined by the formula

$$\phi(x) = \frac{i}{4} \int_{-1}^{1} \frac{k\langle \gamma(t) - x, \nu(t) \rangle}{\|\gamma(t) - x\|} H_1(k\|\gamma(t) - x\|) \rho(t)\, dt, \tag{8}$$

for all $x \in \mathbb{R}^2 \setminus \Gamma$, where $\|\cdot\|$ denotes the Euclidean norm and $\langle \cdot, \cdot \rangle$ denotes the inner product in $\mathbb{R}^2$. Suppose that $g\colon [-1,1] \to \mathbb{C}$ is defined by the formula

$$g(t) = \lim_{\substack{x \to \gamma(t) \\ x \in \Omega_2}} \phi(x), \tag{9}$$

for all $-1 \leq t \leq 1$, i.e. g is the limit of integral (8) when x approaches the point $\gamma(t)$

from inside. It is well known that

$$g(s) = \frac{1}{2}\rho(s) + \frac{i}{4}\int_{-1}^{1} K(t,s)\rho(t)\,dt, \tag{10}$$

for all $-1 \le s \le 1$, where

$$K(t,s) = \frac{k\langle \gamma(t) - \gamma(s), \nu(t)\rangle}{\|\gamma(t) - \gamma(s)\|}\, H_1(k\|\gamma(t) - \gamma(s)\|), \tag{11}$$

for all $-1 \le s, t \le 1$, where $\langle \cdot, \cdot \rangle$ denotes the inner product (see, for example, [20]).

The following theorem is the second of the two principal results of this section. The proof can be found in [25].

Theorem 2.2 *Suppose that N is a positive integer and that ρ is defined by the formula*

$$\rho(t) = \sum_{n=0}^{N} b_n(\mathrm{sgn}(t))^{n+1} J_{\frac{n}{\alpha}}(k|t|) + \sum_{n=0}^{N} c_n(\mathrm{sgn}(t))^n J_{\frac{n}{2-\alpha}}(k|t|), \tag{12}$$

for all $-1 \le t \le 1$, where $b_0, b_1, \ldots, b_N$ and $c_0, c_1, \ldots, c_N$ are arbitrary complex numbers. Suppose further that g is defined by (10). Then there exist series of complex numbers $\beta_0, \beta_1, \ldots$ and $\gamma_0, \gamma_1, \ldots$ such that

$$g(t) = \sum_{n=0}^{\infty} \beta_n |t|^n + \sum_{n=0}^{\infty} \gamma_n\, \mathrm{sgn}(t)|t|^n, \tag{13}$$

for all $-1 \le t \le 1$. Conversely, suppose that g has the form (13). Suppose further that N is an arbitrary positive integer. Then, for all but finitely many angles $\pi\alpha$, there exist complex numbers $b_0, b_1, \ldots, b_N$ and $c_0, c_1, \ldots, c_N$ such that ρ, defined by (12), solves equation (10) to within an error $O(t^{N+1})$.

In other words, if ρ has the form (12), then g is smooth on the intervals $[-1, 0]$ and $[0, 1]$. Conversely, if g is smooth, then for each positive integer N there exists a solution ρ of the form (12) that solves equation (10) to within an error $O(t^{N+1})$.

Remark 2.3 *Suppose that* $G\colon \mathbb{R}^2 \to \mathbb{R}$ *solves the Helmholtz equation on a disc containing the wedge* $\gamma([-1, 1])$*, and that*

$$g(t) = G(\gamma(t)), \tag{14}$$

for all $-1 \leq t \leq 1$*. Suppose further that* N *is an arbitrary positive integer. In [25] we observe that, for* all *angles* $\pi\alpha$*, there exists a function* ρ *of the form (12) solving equation (10) to within an error* $O(t^{N+1})$*.*

Remark 2.4 *The precise relationship between the charge distributions* ρ *of the form (12) and the boundary data* g *in equation (10) is described in detail in Appendix A.*

2.3 The Procedure

Recently, significant progress has been made in the numerical solution of of the boundary integral equations of potential thoery on regions with corners (see, for example, [13], [2]). Essentially the only remaining sticking point is the efficient discretization of the singularities at the corners, which are typically resolved using nested discretizations. We observe that the detailed analysis in this report and the explicit representations (5) and (12) lead to much more efficient discretizations.

For example, in the Neumann case, to resolve the solution in the vicinity of a corner with interior angle $\pi\alpha$, we construct a purpose-made discretization of functions of the

forms

$$\frac{J_{\frac{n}{\alpha}}(kt)}{t}, \tag{15}$$

$$\frac{J_{\frac{n}{2-\alpha}}(kt)}{t}, \tag{16}$$

where $0 \leq t \leq b$ is the distance from the corner, and n is a positive integer (see, for example, [18]). We also construct a quadrature for integrals of the form

$$\int_0^b K(s,t)\,\sigma(s)\,ds, \tag{17}$$

for appropriately chosen t, where K is defined by (4) and σ has the forms (15), (16) (see, for example, [17], [30]). The boundary integral equations are then solved using the Nyström method combined with standard tools. We observe that the condition numbers of the resulting discretized linear systems closely approximate the condition numbers of the underlying physical problems.

Observation 2.5 *While the analysis in this report applies only to polygonal domains, a similar analysis carries over to curved domains with corners. A paper containing the analysis, as well as the corresponding numerical algorithms and numerical examples, is in preparation.*

Observation 2.6 *In the examples in this report, the discretized boundary integral equations are solved in a straightforward manner using standard tools. However, if needed, such equations can be solved much more rapidly using the numerical apparatus from, for example, [24].*

Remark 2.7 *Due to the detailed analysis in this report, the CPU time requirements of the resulting algorithms are almost independent of the requested precision. Thus, in all the examples in this report, the boundary integral equations are solved to essentially full double precision.*

3 The Algorithm

To solve the integral equations of potential theory on polygonal domains, we use a modification of the algorithm described in [2]; instead of discretizing the corner singularities using nested quadratures, we use the representations (5), (12) to construct purpose-made discretizations (see, for example, [18], [17], [30]). A detailed description of this part of the procedure will be published at a later date. The resulting linear systems were solved directly using standard techniques. We illustrate the performance of the algorithm with several numerical examples.

In Table 1, the Neumann and Dirichlet problems were solved on each of the domains in figures 2, 3, 4, 5, where the boundary data were generated by charges *outside* the regions for the exterior problems and *inside* the regions for the interior problems. The numerical solution was tested by doubling the number of nodes near the corners and comparing the computed potentials.

In Table 2, the Neumann and Dirichlet problems were again solved on each of the domains in figures 2, 3, 4, 5, except this time the boundary data were generated by charges *inside* the regions for the exterior problems and *outside* the regions for the interior problems. Since, in this case, the true potentials are avaiable analytically, the numerical solution was tested by comparing the computed potential to the true potential

at several arbitrary points.

In Table 3, we solved the *interior* Dirichlet problem on the relatively simple domains in figures 2, 3, where the boundary data were generated by charges *inside* the regions. We computed the numerical solution using both our algorithm and a naive algorithm which used nested discretizations near the corners. The solution produced by our algorithm was then tested by comparing the computed potentials at several arbitrary points.

Observation 3.1 *It is easy to observe from the values of k and figures 2, 3, 4, and 5 that the regions are between approximately 1 and 15 wavelengths in size. A discussion of the use of these techniques on large-scale problems will be published at a later date. In the examples in tables 2, 1, and 3, k has been chosen so that no resonances, real or spurious, were encountered.*

Observation 3.2 *We observe that if the boundary values are produced by charges* inside *the regions for the exterior problems, or* outside *the regions for the interior problems, then certain terms in the representations of the solutions near the corners vanish. More specifically, in the exterior Neumann case, the terms* $c_1, c_2, \ldots$ *in (5) vanish. In the interior Dirichlet case, the terms* $b_0, b_1, \ldots$ *in (12) vanish.*

4 Extensions and Generalizations

4.1 Other Integral Equations

The apparatus of this report generalizes to other boundary integral equations, such as the combined-potential integral equation (see, for example, [6]) and related situations. This line of investigation is being vigorously pursued.

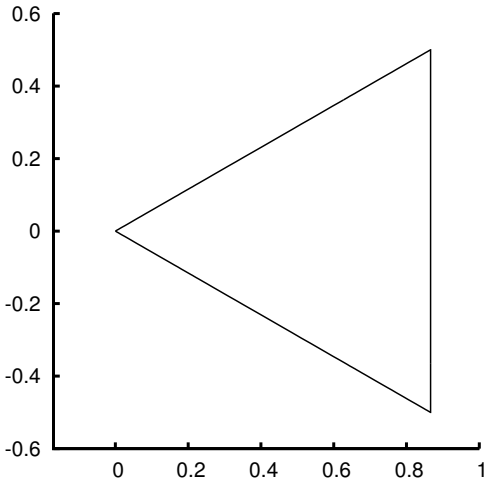

Figure 2: Γ_3: An equilateral triangle in $\mathbb{R}^2$

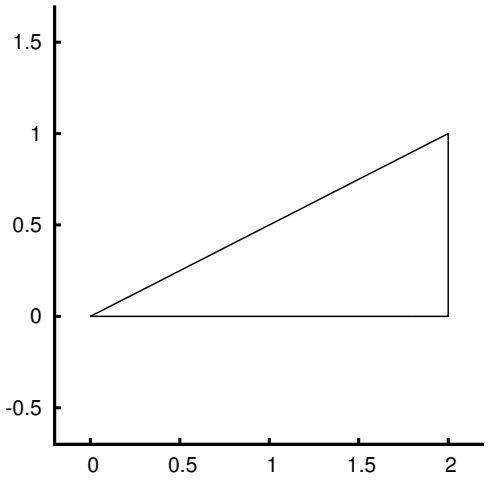

Figure 3: Γ_4: A right triangle in $\mathbb{R}^2$

4.2 Curved Boundaries with Corners

While this report only deals with the solution of the Helmholtz equation on domains with polygonal boundaries, a similar analysis applies to the case of *curved* boundaries with corners. More specifically, if the boundary is smooth except at corners, the solutions to the associated boundary integral equations of potential theory are also representable by series of elementary functions. This analysis, along with the requisite numerical apparatus, will be described in a forthcoming paper.

4.3 Generalization to Three Dimensions

The generalization of the apparatus of this report to three dimensions is fairly straightforward, but the detailed analysis has not been carried out. This line of research is being vigorously pursued.

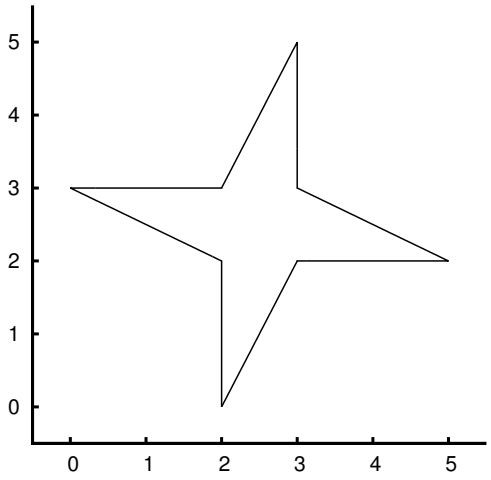

Figure 4: Γ_5: A star-shaped polygon in $\mathbb{R}^2$

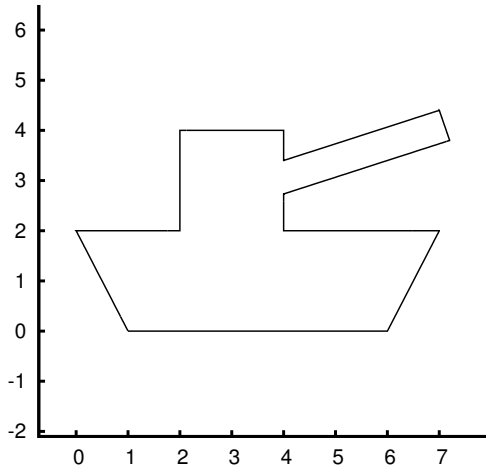

Figure 5: Γ_6: A tank-shaped polygon in $\mathbb{R}^2$

4.4 Robin and Mixed Boundary Conditions

This report deals with the solution of the Helmholtz equation on polygonal domains with either Dirichlet or Neumann boundary conditions. There are two additional boundary conditions that have not yet been analyzed in detail: the Robin condition, which specifies a linear combination of the values of the solution and the values of its derivative on the boundary; and the mixed boundary condition, which specifies Dirichlet boundary conditions on some sides of the polygon and Neumann boundary conditions on others. The results of this investigation will be reported at a later date.

	Boundary curve	k	Number of nodes	Running time	Largest absolute error	Condition number
Interior Neumann problem	Γ_3	17.0	330	0.28642E+00	0.32955E-13	0.26840E+01
	Γ_4	20.0	380	0.53601E+00	0.40764E-12	0.58822E+01
	Γ_5	5.0	968	0.61500E+01	0.36809E-12	0.58674E+01
	Γ_5	15.0	1048	0.78522E+01	0.92945E-12	0.58642E+01
	Γ_6	5.0	1103	0.89752E+01	0.39892E-13	0.21551E+01
	Γ_6	15.0	1233	0.12196E+02	0.47158E-12	0.36966E+01
Exterior Neumann problem	Γ_3	17.0	330	0.32818E+00	0.42646E-15	0.26858E+01
	Γ_4	20.0	380	0.41981E+00	0.33521E-13	0.58866E+01
	Γ_5	5.0	768	0.31816E+01	0.67236E-15	0.58642E+01
	Γ_5	15.0	768	0.31114E+01	0.51226E-13	0.58641E+01
	Γ_6	5.0	1103	0.89982E+01	0.20447E-13	0.21544E+01
	Γ_6	15.0	1103	0.90010E+01	0.38989E-12	0.46689E+01
Interior Dirichlet problem	Γ_3	14.0	252	0.14846E+00	0.41611E-14	0.14278E+02
	Γ_4	20.0	362	0.33653E+00	0.19385E-12	0.27116E+02
	Γ_5	5.0	720	0.26324E+01	0.66780E-14	0.27116E+02
	Γ_5	15.0	800	0.30556E+01	0.14096E-13	0.26880E+02
	Γ_6	5.0	1031	0.72338E+01	0.38829E-12	0.54196E+01
	Γ_6	15.0	1161	0.91036E+01	0.64988E-12	0.89957E+01
Exterior Dirichlet problem	Γ_3	14.0	252	0.14276E+00	0.22170E-13	0.14499E+02
	Γ_4	20.0	362	0.38597E+00	0.46190E-13	0.29318E+02
	Γ_5	5.0	720	0.25672E+01	0.64990E-12	0.52029E+02
	Γ_5	15.0	800	0.31965E+01	0.40631E-12	0.38847E+02
	Γ_6	5.0	1031	0.69795E+01	0.47156E-13	0.73436E+01
	Γ_6	15.0	1031	0.64006E+01	0.83544E-13	0.98740E+01

Table 1: Numerical results for the Helmholtz Neumann and Dirichlet problems, with boundary data produced by charges *inside* for the interior problems, and charges *outside* for the exterior problems. The results were tested by doubling the number of nodes near the corners.

	Boundary curve	k	Number of nodes	Running time	Largest absolute error	Condition number
Interior Neumann problem	Γ_3	17.0	300	0.21332E+00	0.10637E-12	0.26840E+01
	Γ_4	20.0	380	0.51532E+00	0.40858E-14	0.58822E+01
	Γ_5	5.0	888	0.44069E+01	0.77807E-12	0.58678E+01
	Γ_5	15.0	968	0.54840E+01	0.72651E-12	0.58642E+01
	Γ_6	5.0	1103	0.82281E+01	0.19629E-12	0.21551E+01
	Γ_6	15.0	1233	0.10702E+02	0.85866E-13	0.36966E+01
Exterior Neumann problem	Γ_3	17.0	330	0.26114E+00	0.39361E-13	0.26858E+01
	Γ_4	20.0	380	0.47460E+00	0.24299E-13	0.58866E+01
	Γ_5	5.0	768	0.28891E+01	0.21976E-13	0.58642E+01
	Γ_5	15.0	848	0.36247E+01	0.15480E-13	0.58641E+01
	Γ_6	5.0	1233	0.11114E+02	0.26442E-13	0.21544E+01
	Γ_6	15.0	1233	0.10633E+02	0.63324E-12	0.27749E+01
Interior Dirichlet problem	Γ_3	14.0	252	0.13164E+00	0.11935E-14	0.14267E+02
	Γ_4	20.0	362	0.32332E+00	0.17205E-13	0.27116E+02
	Γ_5	5.0	720	0.22676E+01	0.60295E-13	0.27116E+02
	Γ_5	15.0	800	0.32559E+01	0.40323E-13	0.26809E+02
	Γ_6	5.0	1031	0.63333E+01	0.39089E-12	0.54196E+01
	Γ_6	15.0	1161	0.95445E+01	0.16712E-12	0.89957E+01
Exterior Dirichlet problem	Γ_3	14.0	252	0.12741E+00	0.10749E-12	0.14499E+02
	Γ_4	20.0	362	0.37710E+00	0.59616E-13	0.29318E+02
	Γ_5	5.0	720	0.22715E+01	0.43344E-12	0.52029E+02
	Γ_5	15.0	800	0.32999E+01	0.14326E-12	0.38847E+02
	Γ_6	5.0	1031	0.63988E+01	0.26817E-13	0.73436E+01
	Γ_6	15.0	1161	0.97222E+01	0.12680E-12	0.65323E+01

Table 2: Numerical results for the Helmholtz Neumann and Dirichlet problems, with boundary data produced by charges *outside* for the interior problems, and charges *inside* for the exterior problems. The results were tested by comparing the computed potential to the true potential.

	Boundary curve	k	Number of nodes	Running time	Largest absolute error	Condition number
Interior Dirichlet problem	Γ_3	14.0	252	0.18070E+00	0.17986E-13	0.14267E+02
	Γ_4	20.0	362	0.32343E+00	0.76927E-12	0.27116E+02

Table 3: Numerical results for the Helmholtz Neumann and Dirichlet problems on several simple regions, with boundary data produced by charges *inside* for the interior problems, and charges *outside* for the exterior problems. The results were tested by comparing the computed potential to the potential computed by a naïve algorithm.

5 Appendix A

In this section, we describe the precise relationship between the charge distributions ρ of the forms (5), (12) and the boundary data g in equations (3) and (10), in the vicinity of a corner.

5.1 The Neumann Case

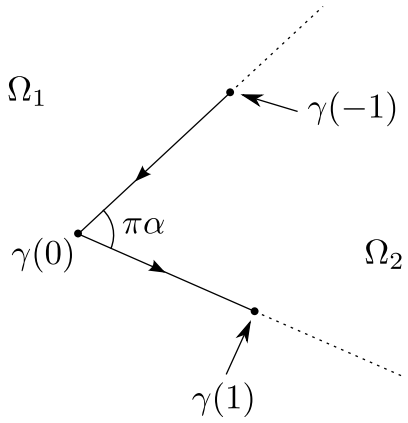

Figure 6: A wedge in $\mathbb{R}^2$

Suppose that $\gamma\colon [-1,1] \to \mathbb{R}^2$ is a wedge in $\mathbb{R}^2$ with a corner at $\gamma(0)$, and with interior angle $\pi\alpha$. Suppose further that γ is parameterized by arc length, and let $\nu(t)$ denote the inward-facing unit normal to the curve γ at t. Let Γ denote the set $\gamma([-1,1])$. By extending the sides of the wedge to infinity, we divide $\mathbb{R}^2$ into two open sets Ω_1 and Ω_2 (see Figure 6).

Let $\phi\colon \mathbb{R}^2 \setminus \Gamma \to \mathbb{C}$ denote the Helmholtz potential (see, for example, [20]) induced by a charge distribution on γ with density $\rho\colon [-1,1] \to \mathbb{C}$. In other words, let ϕ be defined

by (1). Suppose further that $g\colon [-1,1] \to \mathbb{C}$ is defined by (2). It is well known that

$$g(s) = \frac{1}{2}\rho(s) + \frac{i}{4}\int_{-1}^{1} K(s,t)\rho(t)\,dt, \tag{18}$$

for all $-1 \le s \le 1$, where

$$K(s,t) = \frac{k\langle \gamma(s) - \gamma(t), \nu(s)\rangle}{\|\gamma(s) - \gamma(t)\|}\, H_1(k\|\gamma(s) - \gamma(t)\|), \tag{19}$$

for all $-1 \le s,t \le 1$, where $\langle \cdot,\cdot \rangle$ denotes the inner product in $\mathbb{R}^2$.

It is straightforward to show that

$$K(s,t) = \frac{H_1(k\sqrt{s^2+t^2+2st\cos(\pi\alpha)})}{\sqrt{s^2+t^2+2st\cos(\pi\alpha)}} k|t|\sin(\pi\alpha), \tag{20}$$

when both $-1 \le s < 0$ and $0 < t \le 1$, or both $0 < s \le 1$ and $-1 \le t < 0$, and

$$K(s,t) = 0, \tag{21}$$

if either $-1 \le s,t < 0$ or $0 < s,t \le 1$.

In this section, we show that if ρ has the forms

$$\rho(t) = \frac{J_\mu(k|t|)}{|t|}, \tag{22}$$

$$\rho(t) = \mathrm{sgn}(t)\frac{J_\mu(k|t|)}{|t|}, \tag{23}$$

where $\mu > \frac{1}{2}$ is a real number, then, for certain values of μ, the function g defined by (18) is representable by certain series of smooth functions.

The following theorem states that if ρ has the form (22) and $\mu = \frac{2m-1}{\alpha}$ or $\mu = \frac{2m}{2-\alpha}$, where m is an arbitrary positive integer, then g defined by (18) is smooth.

Theorem 5.1 *Suppose that m is a positive integer. Suppose further that $\rho \in L^2([-1,1])$ is defined by the formula*

$$\rho(t) = \frac{J_{\frac{2m-1}{\alpha}}(k|t|)}{|t|}, \tag{24}$$

for all $-1 \leq t \leq 1$. Suppose finally that g is defined by (18). Then

$$g(s) = \frac{1}{2}\sum_{n=1}^{\infty} h_n(\tfrac{2m-1}{\alpha})\,\frac{J_n(k|s|)}{|s|}, \tag{25}$$

for all $-1 \leq s \leq 1$, where $h_n \colon \mathbb{R} \to \mathbb{C}$ is defined by the formula

$$h_n(\nu) = i \cdot n \cdot \sin(\pi\alpha n)\Big(\frac{H_n(k)J_\nu(k)}{n+\nu} - k\frac{H_{n+1}(k)J_\nu(k) - H_n(k)J_{\nu+1}(k)}{n^2-\nu^2}\Big), \tag{26}$$

for all real ν and all positive integers n, where $\pi\alpha$ is the angle at the corner (see Figure 6).

Likewise, if

$$\rho(t) = \frac{J_{\frac{2m}{2-\alpha}}(k|t|)}{|t|}, \tag{27}$$

for all $-1 \leq t \leq 1$ and g is defined by (18), then

$$g(s) = \frac{1}{2}\sum_{n=1}^{\infty} h_n(\tfrac{2m}{2-\alpha})\,\frac{J_n(k|s|)}{|s|}, \tag{28}$$

for all $-1 \leq s \leq 1$, where h_n is defined by (26).

The following theorem states that if ρ has the form (23) and $\mu = \frac{2m}{\alpha}$ or $\mu = \frac{2m-1}{2-\alpha}$, where m is an arbitrary positive integer, then g defined by (18) is smooth.

Theorem 5.2 *Suppose that m is a positive integer. Suppose further that $\rho \in L^2([-1,1])$ is defined by the formula*

$$\rho(t) = \operatorname{sgn}(t) \frac{J_{\frac{2m}{\alpha}}(k|t|)}{|t|}, \tag{29}$$

for all $-1 \leq t \leq 1$. Suppose finally that g is defined by (18). Then

$$g(s) = -\frac{1}{2} \sum_{n=1}^{\infty} h_n(\tfrac{2m}{\alpha}) \operatorname{sgn}(s) \frac{J_n(k|s|)}{|s|}, \tag{30}$$

for all $-1 \leq s \leq 1$, where h_n is defined by (26).

Likewise, if

$$\rho(t) = \operatorname{sgn}(t) \frac{J_{\frac{2m-1}{2-\alpha}}(k|t|)}{|t|}, \tag{31}$$

for all $-1 \leq t \leq 1$ and g is defined by (18), then

$$g(s) = -\frac{1}{2} \sum_{n=1}^{\infty} h_n(\tfrac{2m-1}{2-\alpha}) \operatorname{sgn}(s) \frac{J_n(k|s|)}{|s|}, \tag{32}$$

for all $-1 \leq s \leq 1$, where h_n is defined by (26).

5.2 The Dirichlet Case

Suppose that $\gamma\colon [-1,1] \to \mathbb{R}^2$ is a wedge in $\mathbb{R}^2$ with a corner at $\gamma(0)$, and with interior angle $\pi\alpha$. Suppose further that γ is parameterized by arc length, and let $\nu(t)$ denote

the inward-facing unit normal to the curve γ at t. Let Γ denote the set $\gamma([-1,1])$. By extending the sides of the wedge to infinity, we divide $\mathbb{R}^2$ into two open sets Ω_1 and Ω_2 (see Figure 6).

Let $\phi\colon \mathbb{R}^2\setminus\Gamma \to \mathbb{C}$ denote the Helmholtz potential (see, for example, [20]) induced by a dipole distribution on γ with density $\rho\colon [-1,1]\to\mathbb{C}$. In other words, let ϕ be defined by (8). Suppose further that $g\colon [-1,1]\to\mathbb{C}$ is defined by (9). It is well known that

$$g(s) = \frac{1}{2}\rho(s) + \frac{i}{4}\int_{-1}^{1} K(t,s)\rho(t)\,dt, \tag{33}$$

for all $-1 \le s \le 1$, where

$$K(t,s) = \frac{k\langle \gamma(t)-\gamma(s), \nu(t)\rangle}{\|\gamma(t)-\gamma(s)\|}\, H_1(k\|\gamma(t)-\gamma(s)\|), \tag{34}$$

for all $-1 \le s,t \le 1$, where $\langle\cdot,\cdot\rangle$ denotes the inner product in $\mathbb{R}^2$.

It is straightforward to show that

$$K(t,s) = \frac{H_1(k\sqrt{s^2+t^2+2st\cos(\pi\alpha)})}{\sqrt{s^2+t^2+2st\cos(\pi\alpha)}} k|s|\sin(\pi\alpha), \tag{35}$$

when both $-1 \le s < 0$ and $0 < t \le 1$, or both $0 < s \le 1$ and $-1 \le t < 0$, and

$$K(t,s) = 0, \tag{36}$$

if either $-1 \le s,t < 0$ or $0 < s,t \le 1$.

In this section, we show that if ρ has the forms

$$\rho(t) = J_\mu(k|t|), \tag{37}$$

$$\rho(t) = \operatorname{sgn}(t) J_\mu(k|t|), \tag{38}$$

where $\mu > \frac{1}{2}$ is a real number, then, for certain values of μ, the function g defined by (33) is representable by certain series of smooth functions.

The following theorem states that if ρ has the form (37) and $\mu = 0$ or $\mu = \frac{2m-1}{\alpha}$ or $\mu = \frac{2m}{2-\alpha}$, where m is an arbitrary positive integer, then g defined by (33) is smooth.

Theorem 5.3 *Suppose that m is a positive integer. Suppose further that $\rho \in L^2([-1,1])$ is defined by the formula*

$$\rho(t) = J_{\frac{2m-1}{\alpha}}(k|t|), \tag{39}$$

for all $-1 \le t \le 1$. Suppose finally that g is defined by (33). Then

$$g(s) = \frac{1}{2} \sum_{n=1}^{\infty} h_n(\tfrac{2m-1}{\alpha})\, J_n(k|s|), \tag{40}$$

for all $-1 \le s \le 1$, where h_n is defined by formula (26).

Likewise, if

$$\rho(t) = J_{\frac{2m}{2-\alpha}}(k|t|), \tag{41}$$

for all $-1 \leq t \leq 1$ *and* g *is defined by (33), then*

$$g(s) = \frac{1}{2} \sum_{n=1}^{\infty} h_n(\tfrac{2m}{2-\alpha})\, J_n(k|s|), \tag{42}$$

for all $-1 \leq s \leq 1$*, where* h_n *is defined by (26).*

Finally, if

$$\rho(t) = J_0(k|t|), \tag{43}$$

for all $-1 \leq t \leq 1$ *and* g *is defined by (33), then*

$$g(s) = \frac{2-\alpha}{2} J_0(k|s|) + \frac{1}{2} \sum_{n=1}^{\infty} h_n(0)\, J_n(k|s|), \tag{44}$$

for all $-1 \leq s \leq 1$*, where* h_n *is defined by (26).*

The following theorem states that if ρ has the form (38) and $\mu = 0$ or $\mu = \frac{2m}{\alpha}$ or $\mu = \frac{2m-1}{2-\alpha}$, where m is an arbitrary positive integer, then g defined by (33) is smooth.

Theorem 5.4 *Suppose that* m *is a positive integer. Suppose further that* $\rho \in L^2([-1,1])$ *is defined by the formula*

$$\rho(t) = \operatorname{sgn}(t) J_{\frac{2m}{\alpha}}(k|t|), \tag{45}$$

for all $-1 \leq t \leq 1$*. Suppose finally that* g *is defined by (33). Then*

$$g(s) = -\frac{1}{2} \sum_{n=1}^{\infty} h_n(\tfrac{2m}{\alpha})\, \operatorname{sgn}(s) J_n(k|s|), \tag{46}$$

for all $-1 \leq s \leq 1$, *where* h_n *is defined by (26).*

Likewise, if

$$\rho(t) = \operatorname{sgn}(t) J_{\frac{2m-1}{2-\alpha}}(k|t|), \tag{47}$$

for all $-1 \leq t \leq 1$ *and* g *is defined by (33), then*

$$g(s) = -\frac{1}{2} \sum_{n=1}^{\infty} h_n(\tfrac{2m-1}{2-\alpha}) \operatorname{sgn}(s) J_n(k|s|), \tag{48}$$

for all $-1 \leq s \leq 1$, *where* h_n *is defined by (26).*

Finally, if

$$\rho(t) = \operatorname{sgn}(t) J_0(k|t|), \tag{49}$$

for all $-1 \leq t \leq 1$ *and* g *is defined by (33), then*

$$g(s) = \frac{\alpha}{2} \operatorname{sgn}(t) J_0(k|s|) - \frac{1}{2} \sum_{n=1}^{\infty} h_n(\tfrac{2m-1}{2-\alpha}) \operatorname{sgn}(s) J_n(k|s|), \tag{50}$$

for all $-1 \leq s \leq 1$, *where* h_n *is defined by (26).*

References

[1] Abramowitz, Milton, and Irene A. Stegun, eds. *Handbook of Mathematical Functions With Formulas, Graphs, and Mathematical Tables.* Washington: U.S. Govt. Print. Off., 1964.

[2] Bremer, James. "A fast direct solver for the integral equations of scattering theory on planar curves with corners." *J. Comput. Phys.* 231 (2012): 1879–1899.

[3] Calderón, A. P., C. P. Calderón, E. Fabes, M. Jodeit, and N. M. Riviere. "Applications of the Cauchy Integral on Lipschitz Curves." *B. Am. Math. Soc.* 84.2 (1978): 287–290.

[4] Carleson, L. "On the Support of Harmonic Measure for Sets of Cantor Type." *Ann. Acad. Sci. Fenn.* 10 (1985): 113–123.

[5] Coifman, R. R., Peter W. Jones, and Stephen Semmes. "Two elementary Proofs of the L^2 Boundedness of Cauchy Integrals on Lipschitz Curves." *J. Am. Math. Soc.* 2.3 (1989): 553–564.

[6] Colton, D. and R. Kress. *Inverse Acoustic and Electromagnetic Scattering Theory.* 3rd ed. New York: Springer, 2013.

[7] Courant, R. and D. Hilbert. *Methods of Mathematical Physics.* New York: Interscience Publishers, 1966.

[8] Golub, Gene H. and Charles F. Van Loan. *Matrix Computations.* 4th ed. Baltimore: The Johns Hopkins University Press, 2013.

[9] Gradshteyn, I. S., and I. M. Ryzhik. *Table of Integrals, Series, and Products.* 7th ed. Eds. Alan Jeffrey and Daniel Zwillinger. San Diego: Academic Press, 2000.

[10] Greengard, Leslie, and Vladimir Rokhlin. "A fast algorithm for particle simulations." *J. Comput. Phys.* 73.2 (1987): 325–348.

[11] Grisvard, Pierre. *Elliptic problems in nonsmooth domains.* Boston: Pitman Advanced Pub. Program, 1985.

[12] Hao, S., A. H. Barnett, P. G. Martinsson, and P. Young. "High-order accurate Nyström discretization of integral equations with weakly singular kernels on smooth curves in the plane." it Adv. Comput. Math. 40 (2014)

[13] Helsing, J. and R. Ojala. "Corner singularities for elliptic problems: integral equations, graded meshes, quadrature, and compressed inverse preconditioning." *J. Comput. Phys.* 227 (2008): 8820–8840.

[14] Jerison, David S., and Carlos E. Kenig. "The Neumann Problem on Lipschitz Domains." *B. Am. Math. Soc.* 4.2 (1981): 203–207.

[15] Jones, P., J. Ma, and V. Rokhlin. "A fast direct algorithm for the solution of the Laplace equation on regions with fractal boundaries." *J. Comput. Phys.* 113.1 (1994): 35–51.

[16] Lehman, R. Sherman. "Development of the Mapping Function at an Analytic Corner." *Pacific Journal of Mathematics* 7.3 (1957): 1437–1449.

[17] Ma, J., V. Rokhlin, and S. Wandzura. "Generalized Gaussian Quadrature Rules for Systems of Arbitrary Functions." *SIAM. J. Numer. Anal.* 33.3 (1996): 971–996.

[18] Martinsson, Per-Gunnar, Vladimir Rokhlin, and Mark Tygert. "On Interpolation and Integration in Finite-Dimensional Spaces of Bounded Functions." *Comm. App. Math. and Comp. Sci.* 1.1 (2006): 133–142.

[19] Maz'ya, V. G. and S. M. Nikol'skii, eds. *Analysis IV: Linear and Boundary Integral Equations (Encycopedia of Mathematical Sciences).* Trans. A. Böttcher and S. Prössdorf. New York: Springer-Verlag, 1991.

[20] Mikhlin, S. G. *Integral Equations.* New York: Pergamon Press, 1957.

[21] Petrovsky, I. G. *Lectures on Partial Differential Equations.* 4th printing. New York: Interscience Publishers, 1954.

[22] R. J. Riddell, Jr. "Boundary-Distribution Solution of the Helmholtz Equation for a Region with Corners." J. Comput. Phys. 31 (1979): 21–41.

[23] Rokhlin, V. "Rapid Solution of Integral Equations of Classical Potential Theory." *J. Comput. Phys.* 60 (1983): 187–207.

[24] Rokhlin, Vladimir. "Rapid solution of integral equations of scattering theory in two dimensions." *Journal of Computational Physics* 86.2 (1990): 414–439.

[25] Serkh, Kirill. "On the Solution of Elliptic Partial Differential Equations on Regions with Corners." *Yale Technical Report YALEU/DCS/TR-1523* (2016).

[26] Trefethen, Lloyd N. "Numerical Computation of the Schwarz-Christoffel Transformation." *SIAM J. Sci. Stat. Comput.* 1.1 (1980): 82–102.

[27] Verchota, Gregory. "Layer Potentials and Regularity for the Dirichlet Problem for Laplace's equation in Lipschitz Domains." *J. Funct. Anal.* 59 (1984): 572–611.

[28] Wolfgang Wasow. "Asymptotic Development of the Solution of Dirichlet's Problem at Analytic Corners." Duke Math. J. 24 (1957): 47–56.

[29] Wigley, Neil M. "On a method to subtract off a singularity at a corner for the Dirichlet or Neumann problem." *Mathematics of Computation* 23.106 (1969): 395–401.

[30] Yarvin, N. and V. Rokhlin. "Generalized Gaussian Quadratures and Singular Value Decompositions of Integral Operators." *SIAM J. Sci. Comput.* 20.2 (1998): 699–718.

[31] Zargaryan, S. S., and V. G. Maz'ya. "The Asymptotic Form of the Solutions of the Integral Equations of Potential Theory in the Neighborhood of the Corner Points of a Contour." *PMM U.S.S.R.* 48.1 (1984): 120–124.